Materials & Design 219 (2022) 110787

Contents lists available at ScienceDirect

Materials & Design

journal homepage: www.elsevier.com/locate/matdes

Self-sensing composite material based on piezoelectric nanofibers

Giacomo Selleri [a,*], Maria Elena Gino [b,*], Tommaso Maria Brugo [c], Riccardo D'Anniballe [d], Johnnidel Tabucol [c], Maria Letizia Focarete [b], Raffaella Carloni [d], Davide Fabiani [a], Andrea Zucchelli [c]

[a] Department of Electrical, Electronic, and Information Engineering, University of Bologna, Viale Risorgimento 2, 40136 Bologna, Italy
[b] Department of Chemistry "Giacomo Ciamician" and INSTM UdR of Bologna, University of Bologna, via Selmi 2, 40126 Bologna, Italy
[c] Department of Industrial Engineering, University of Bologna, Viale Risorgimento 2, 40136 Bologna, Italy
[d] Faculty of Science and Engineering – Bernoulli Institute for Mathematics, Computer Science and Artificial Intelligence, University of Groningen, Nijenborgh 9 9747 AG, Groningen, the Netherlands

HIGHLIGHTS

- Polymeric piezoelectric nanofibers were successfully embedded in a composite laminate for self-sensing applications.
- Using an analytical model, the circuit parameters are adapted to make the sensor capable of monitoring quasi-static loads.
- The sensitivity of the self-sensing laminate is preserved after 10^6 cycles of compressive fatigue tests.
- The nanofibers integration with the composite laminate does not affect its mechanical strength, avoiding delamination risks.

GRAPHICAL ABSTRACT

ARTICLE INFO

Article history:
Received 3 January 2022
Revised 25 May 2022
Accepted 25 May 2022
Available online 30 May 2022

Keywords:
Composite
Poly(vinylidenefluoride-trifluoroethylene) (PVDF-TrFE)
Piezoelectric
Flexible sensor
Smart material

ABSTRACT

Recently, efforts have been made to manufacture self-sensing smart composites by integrating piezoelectric sensors with laminates. However, the interleaving of pressure sensors, such as piezoelectric polymeric films, dramatically reduces the impact resistance of the hosting laminates, and consequently, delamination can occur. This study aimed to fabricate a self-sensing composite material by embedding piezoelectric nanofibers of poly(vinylidenefluoride-trifluoroethylene) (PVDF-TrFE) in a polymeric elastic matrix and carbon black-based electrodes to detect a piezoelectric signal. The mechanical and electrical properties of the self-sensing laminate were maintained after 10^6 fatigue test cycles. By appropriately tuning the parameters of the acquisition circuit, the sensor could measure not only impulsive loads but also low-frequency loads as low as 0.5 Hz. A piezoelectric model with lumped parameters for the polarization process and piezoelectric response of the nanofibers is proposed and validated by experimental results. As a proof of the model, the piezoelectric nanofiber sensors were embedded in a prosthetic carbon fiber sole, and the piezoelectric signal response closely followed the ground reaction force with a sensitivity of 0.14 mV/N.

1. Introduction

Owing to their lightweight structure and high mechanical performance, fiber-reinforced plastics (FRP) are key components in a

* Corresponding authors.
E-mail addresses: giacomo.selleri2@unibo.it (G. Selleri), mariaelena.gino2@unibo.it (M.E. Gino).

https://doi.org/10.1016/j.matdes.2022.110787
0264-1275/

wide range of industrial applications, including civil engineering, aerospace, and automotive applications. However, their laminar morphology can lead to mechanical damage or delamination in the case of high or out-of-plane loads. To monitor and prevent failure of the component, non-destructive structural health monitoring (SHM) sensors (e.g., piezoelectric, resistive, or capacitive sensors) have been either installed on the surface of the material or integrated within the laminate structure [1,2].

Self-sensing composite laminates are smart materials that can perform real-time in situ SHM, which broadens their use in other application domains, such as robotics, wearable devices, and prosthetic systems [3,4,5,6], in which lightweight, flexible pressure sensors can ensure high-precision contact detection and a good estimation of the ground morphology.

A variety of sensors have been investigated based on their sensing mechanisms, and their sensitivity, sensing range, linearity, and life cycle have been evaluated. For instance, the working principle of piezoresistive sensors is based on the variation in the electrical resistance of a material as a result of its deformation. When pressure is applied to a semi-conductive material (e.g., carbon fiber-based composite materials, carbon-based nanomaterials, or conductive polymers [7]), the change in its electrical conductivity is converted into an output voltage. Research on capacitive sensing mechanisms has focused on highly sensitive flexible structures and capacitive-based pressure sensors [8]. When an external force is applied perpendicular to the sensor, the variation in the distance between the electrodes leads to a change in the capacitance. The sensitivity and sensing limits of capacitive sensors depend on the elasticity of the dielectric films used, such as polydimethylsiloxane (PDMS) or Ecoflex [9,10]. By filling the elastic matrix with conductive nanoparticles (e.g., carbon black or graphite), the mechanical strength and electrical conductivity of the composite material are enhanced, resulting in a high sensitivity and a wide sensing range [11].

Despite their good performance, these pressure sensors usually rely on an external power supply, which leads to problems owing to the need for periodic battery replacement and structural complexity. For this reason, triboelectric devices have recently shown optimal performance for signal generation, particularly for energy harvesting [12,13]. However, their working mechanisms are not suitable for SHM systems or for integration into composite laminates. Moreover, piezoelectric materials have attracted enormous interest due to their self-powering capability during their transducing mechanisms. Based on their conversion efficiencies, they are considered suitable for various purposes. For example, ceramic piezoelectric materials (e.g., lead zirconate titanate (PZT)) exhibit a high piezoelectric response and are widely used in energy harvesting applications [14]. However, piezoelectric polymers (e.g., polyvinylidene fluoride PVDF and its copolymers) are often preferred for mechanical sensing applications because of their ability to be fabricated in the form of thin films, even though they have a lower piezoelectric coefficient [15,16]. Efforts have been made to combine the flexibility of piezoelectric polymers with the high coefficients of piezoceramic materials. For example, PZT nanofibers have been used as fillers for PVDF films [17] and composite nanofibers based on barium zirconate titanate–barium calcium titanate (BZT–BCT) and PVDF have been electrospun [18].

In a self-sensing composite material, the integration of external sensors could be a suitable solution to avoid changes in the mechanical performance of composite laminates. However, exposure to external environmental conditions or electrical noise could lead to damage and shorten life cycles. To overcome these problems, several studies have been conducted on the possibility of embedding pressure sensors between laminate piles [19,20]. On the one hand, the PZT disk is considered a promising solution owing to its high piezoelectric coefficient, but its fragile and brittle nature could lead to mechanical delamination in the case of PZT fracture. On the other hand, flexible piezopolymers such as PVDF are good alternatives, despite having lower piezoelectric coefficients. However, the interfacial strength between the polymer film and hosting matrix can still lead to mechanical delamination during out-of-plane impacts. Moreover, the addition of traditional metal electrodes for signal detection leads to a discontinuity in the structure of the composite material.

In this study, a nanofiber piezoelectric membrane of poly(vinyli denefluoride-trifluoroethylene) (PVDF-TrFE) obtained via electrospinning was embedded in a polymeric matrix to fabricate a flexible piezoelectric sensor that could be integrated into a composite material. The intimate contact between the nanofibers and the surrounding matrix prevented the risk of delamination and increased the impact resistance of the composite material [21,22]. In addition, a specific type of electrode was proposed in which conductive carbon nanopowders were dispersed in the same material that the nanofibers were hosted in to avoid material discontinuities and prevent mechanical failures [23,24,25]. Typically, piezoelectrics are used for dynamic stress detection, for example, impact detection in SHM systems or vibrations [26]. In this study, a suitable signal conditioning system was proposed to achieve optimal signal detection performance, even for low-frequency loads. As a proof of concept, a biomedical application, ground reaction force detection during the gait cycle in a transfemoral prosthetic leg, was selected for the developed self-sensing composite material. In general, the flexibility of such piezoelectric devices can be used to fabricate self-sensing materials with special shapes or curvilinear structures, for example, for the steering wheel of a car or for sole sensing.

2. Materials and methods

The fabrication process of the nanofiber piezoelectric flexible sensor is described in Sections 2.1–2.4. The electrospinning process, polarization of the nanofibers, integration of the nanofiber membrane with an elastic polymeric matrix, and the manufacture of the electrodes are also explained in these sections. Section 2.5 then describes the integration of the piezoelectric sensor into a composite material.

2.1. Electrospinning process

The piezoelectric nanofiber mat was produced via electrospinning, starting from a polymeric solution prepared by dissolving 7 wt% of the copolymer PVDF-TrFE (80/20 mol%, M_w = 600 kDa, kindly provided by Solvay S.p.A. Milan, Italy, https://www.solvay.-com) in dimethylformamide (DMF) (23 wt%) and acetone (AC) (70 wt%). The PVDF-TrFE exhibited a Curie temperature of 133 °C and a melting point of 145 °C. The electrospinning process was performed in a Spinbow Lab Unit (Spinbow S.r.l., Bologna, Italy) by applying 15 kV to the high-voltage needle and collecting the randomly oriented nanofibers on a grounded rotating drum (0.2 m/s tangential velocity) at 20–25 °C and 40–50% relative humidity (RH). The process was performed for 2 h at 0.8 ml/h a flow rate.

2.2. Piezoelectric nanofiber polarization process

The high electric field of the electrospinning process promotes the formation of the polar β-phase in PVDF-TrFE, which is responsible for its piezoelectric behavior. Nevertheless, a poling process is required to fully align the ferroelectric domains of the nanofibers by applying an external electric field [27]. Because the highly porous nanofiber layer is located between the high-voltage electrode and the ground electrode, the electric field is distributed unevenly

on the nanofibers and the embedding medium according to their electrical properties, unlike a bulk sample (such as a PVDF-TrFE film), where the electric field is applied directly to it [28,29]. In particular, the electric-field distribution on each material during the polarization process depends on its permittivity and conductivity [30,31].

The schematic representation of the polarization process in Fig. 1a can be modeled as a multilayer system whose equivalent electrical circuit is shown in Fig. 1b, where the nanofibers (*nf*) and embedding medium (*em*) are represented as *n*-times the series of their resistance (R_{nf}, R_{em}) and capacitance (C_{nf}, C_{em}). The resistance R_i is the opposite of the conductance G_i ($R_i = 1/G_i$), where G_i is proportional to the conductivity σ_i and capacitance C_i is proportional to the permittivity ε_i.

When the DC voltage generator is switched on, the first transient domain distributes the electric field on different materials according to their permittivity (ε). However, in the steady-state domain, which is reached after a certain time τ [32], the electric field distribution is determined by the conductivity values (σ) of the materials (i.e., higher on the material with lower conductivity). By schematizing the composite as a two-layer system, the time constant τ can be calculated as described in Equation (1):

$$\tau = \tau_{nf} * \tau_{em} * \frac{\frac{1}{\varepsilon_{nf}} + \frac{h}{\varepsilon_{em}}}{\frac{1}{\sigma_{nf}} + \frac{h}{\sigma_{em}}} \quad (1)$$

where $h = h_{em}/h_{nf}$ and $\tau_i = \varepsilon_i/\sigma_i$. h_{em} and h_{nf} represent the thicknesses of the embedding medium and nanofibers, respectively. By neglecting, after a period of 10 τ, the capacitors C_{nf} and C_{em}, the electric field applied to the nanofibers (E_{nf}) can be simply calculated using Equation (2), where E is the electric field applied (with the voltage generator) to the whole system and h_{tot} is the total thickness (100 μm) [30].

$$E_{nf} = \frac{\frac{Eh_{tot}}{\sigma_{nf}}}{\frac{h_{nf}}{\sigma_{nf}} + \frac{h_{em}}{\sigma_{em}}} \quad (2)$$

In this study, a vegetable oil (FR3 natural ester, Cargill) with a breakdown voltage of 70 kV/mm and an electrical conductivity σ_{em} of 9.8 * 10^{-10} S/m measured at 130 °C was used for the polarization process. This oil was chosen after a detailed study of a wide range of embedding media (i.e., epoxy resin, silicon rubber, air, vegetable oil, silicone oil, and seed oil), considering their electrical conductivity and breakdown voltage [31]. The polarization temperature was set to the Curie temperature (130 °C) to facilitate dipole orientation in the electric field direction. Considering a PVDF-TrFE conductivity σ_{nf} = 6,24 * 10^{-10} S/m (measured at 130 °C), h_{nf}= 40 μm, h_{em}=60 μm, and setting the electric field E to 30 kV/mm using a DC voltage generator (Keithley 2290E-5), the electric field on the nanofibers E_{nf} was calculated to be 25 kV/mm. According to Equation (1), it was possible to calculate τ on the order of 0.1 s (ε_{nf} = 11 and ε_{em} = 4), so the process took place in an oil bath for 5 min (>10 τ), in the steady-state regime of the electric field distribution. The electric field was maintained constant until the oil cooled to room temperature. Finally, the nanofiber layer was immersed in a cyclohexane bath for 1 h to remove the oil completely.

The amplitude of the electric field used to polarize the nanofiber mat was chosen as a result of an investigation of a 100 μm thick commercial film of PVDF-TrFE film (80/20 mol%). The bulk commercial film was polarized at different electric field amplitudes at a temperature of 130 °C. After each polarization, the piezoelectric strain coefficient d_{33} was measured using a piezometer (d_{33} PiezoMeter System, Piezotest, Singapore, https://www.piezotest.com). As observed in Fig. 2, the d_{33} shows an increasing trend for low values of the electric polarization field before stabilizing at a regime value of −27 pC/N for electric fields above 7 kV/mm.

Therefore, in the case of the PVDF-TrFE nanofiber mat, an electric field of 25 kV/mm was a sufficient value for complete polarization at 130 °C. Before the polarization, the d_{33} value of the nanofibers was measured to be close to zero, while after the process, it increased up to −13 pC/N, a value comparable to that of the commercial thin film of PVDF-TrFE (-27 pC/N).

2.3. Piezoelectric nanofiber integration

After the piezoelectric properties of the nanofibers were optimized and the original porosity level was restored by removing the oil, the nanofiber membrane could be integrated with a hosting material such as epoxy resin or silicone rubber. To interleave the piezoelectric sensor in the composite laminate (Section 2.5), the embedding medium of the nanofibers was chosen to be compatible with the epoxy resin of the composite material. To fit the sensor into curvilinear geometries and avoid introducing brittle components into the system, good flexibility of the device was achieved by embedding the nanofiber layer in a mixture of epoxy resin (Itapox 108, kindly provided by Ddchem S.l.r., Verona, Italy) (55 wt%) and blocked isocyanate polyurethane prepolymer (Synthane 2095, Synthesia Technology, Barcelona, Spain) (24 wt%). A curing agent (Itamine CA119, Ddchem S.l.r., Verona, Italy) was then added (21 wt%). Polyurethane was added to the epoxy resin to increase the elasticity of the matrix while ensuring good adhesion to the laminate resin. The nanofiber membrane was placed on a PTFE

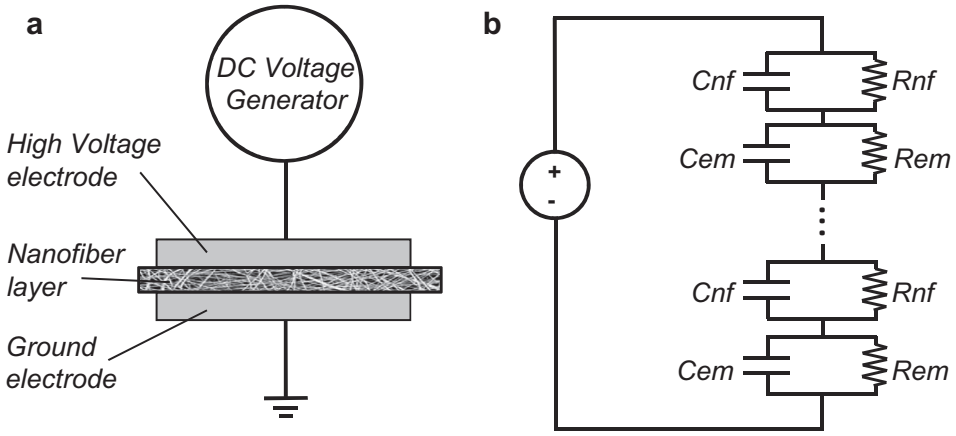

Fig. 1. (a) A schematic representation of the piezoelectric nanofiber polarization process; (b) the equivalent circuit of the polarization process.

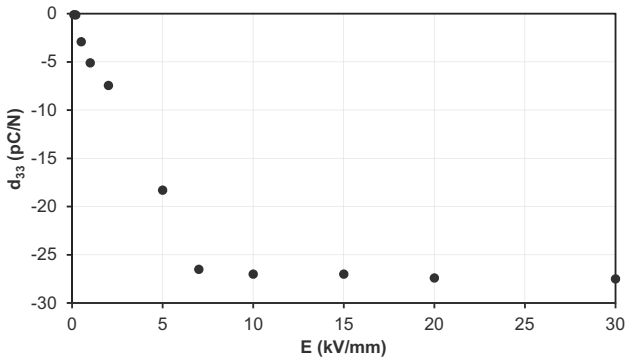

Fig. 2. The piezoelectric strain coefficient d_{33} vs poling electric polarization field at 130 °C.

support and surrounded by a 100 μm thick casting mask (Fig. 4a). As the mixture was poured onto the nanofiber substrate (Fig. 4b), the pores were filled, and the nanofibers were integrated. Excess material was removed from the surface of the layer using a blade, as shown schematically in Fig. 4c [24]. The material was cured at 50 °C for 2 h.

2.4. Electrode manufacturing

Although conventional metal electrodes guarantee high conductivity, the introduction of material discontinuities into composite laminates can lead to mechanical delamination. In addition, metallic electrodes such as aluminum foils or gold-sputtered layers have a limited maximum strain before breakage and would limit the flexibility of the sensor. To overcome these problems, electrodes were fabricated by dispersing conductive carbon black (CB) nanoparticles in the same material used to integrate the nanofibers. Doing so avoided problems related to the interleaving of metal electrodes, and the elimination of any material interruptions improved the adhesion between the electrodes and the piezoelectric layer. When carbon black nanoparticles are mixed into a polymer matrix, their high specific surface area can form a conductive network that significantly increases the conductivity of the resin, even when only a small amount of nanoparticles is added [33].

In this study, 10 wt% conductive nanoparticles of carbon black (CB, Printex XE2B, BET surface area = 1000 m^2/g, average particle size = 30 nm) were added to a mixture of epoxy resin and polyurethane (90 wt%), as described in Section 2.3, to fabricate the electrodes of the piezoelectric sensor.

Preliminary studies were performed to estimate the conductivity of the nano-filled resin as a function of the CB content. Different

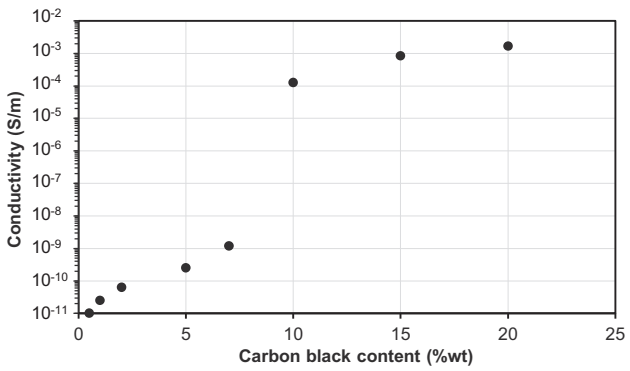

Fig. 3. The electrical conductivity of the electrodes as a function of the Carbon Black (CB) content.

layers were prepared with different amounts of CB, and their electrical conductivities were measured, as shown in Fig. 3. The electrical conductivity gradually increased at low values of CB before sharply rising when the percolation threshold was attained, corresponding to a specific CB content (7 wt%) [34].

To manufacture the electrodes of the piezoelectric sensor, 10 wt % of CB nanoparticles were added to a mixture of epoxy resin and polyurethane (90 wt%), providing an electrical conductivity of 1.25 * 10^{-4} S/m. The liquid formulation was prepared by adding isopropanol (300 wt%) and magnetically stirring for 120 h at room temperature. This solution was deposited on the surface of the piezoelectric layer at 40 °C for 20 min to allow the isopropanol to evaporate, as shown in Fig. 4d. A homogeneous layer of 100 μm thickness was prepared using a blade and cured for 2 h at 50 °C (Fig. 4e). This process was repeated for the opposite electrode surfaces. Signal cables (430-FST, Micro-Measurements, Raleigh, NC 27611, USA, https://www.micro-measurements.com) coated with a Teflon jacket were placed within the electrode layers during the curing process. The total thickness of the sensor shown in Fig. 4f was approximately 300 μm. The signal-to-noise ratio can deteriorate owing to external phenomena such as triboelectricity effects; to reduce the external electrical noise, shield electrodes were added to the structure of the sensor using the same fabrication process used for the signal electrodes (Fig. 4g).

2.5. Self-sensing composite material stacking sequence

The piezoelectric sensor was integrated with a carbon fiber reinforced polymer (CFRP) precured laminate with a quasi-isotropic stacking sequence $[0/\pm45/90]_s$ and dimensions of 100 × 50 × 3 mm. A layer of glass fiber reinforced polymer (GFRP) prepreg (E-glass 8H balanced Satin 300 g/m^2 - epoxy matrix, VV300S - DT121H-34 DeltaPreg, 80 × 90 × ~0.22 mm) was stacked on the CFRP precured laminate, with a 0° orientation. The piezoelectric sensor was then placed on top and finally covered with another GFRP prepreg ply oriented at 0°, as depicted in Fig. 5. The GFRP layer under the piezoelectric sensor electrically insulates it from the conductive CFRP base, while the GFRP layer covering the sensor protects it from triboelectric effects and electromechanical noise that negatively affect the piezoelectric signal. Before stacking, the surface of the CFRP base was ground with sandpaper (P220) to improve adhesion with the resin of the GFRP layer. The curing process was then performed in a vacuum bag for 12 h at 80 °C. The integration of the sensor with the plane CFRP sheet was performed to perform standard compression tests for comprehensive electromechanical characterization prior to the fabrication of complex geometries, such as a prosthetic foot sole.

2.6. Characterization techniques

The morphology of the electrospun fibers and their impregnation in the hosting material were studied using a Phenom Pro X scanning electron microscope (SEM). Samples were sputter-coated with gold prior to the examination, and the distribution of fiber diameters was determined by measuring approximately 100 fibers using an image analysis software (ImageJ). After polishing, a cross-sectional evaluation of the self-sensing laminate was performed using optical micrograph analysis.

X-ray diffraction (XRD) measurements were carried out using an X'PERT pro Instrument, with detector 1-D PIXcell using Cu radiation 1.54 Å, as reported in Appendix A.

The piezoelectric signal response was investigated in the frequency range of 0.25–20 Hz using a tensile machine ElectroPuls E1000 (Instron™, Norwood (MA), USA, https://www.instron.us) equipped with a 2 kN load cell. The self-sensing laminate was compressed between a flat plate and cylindrical indenter with a

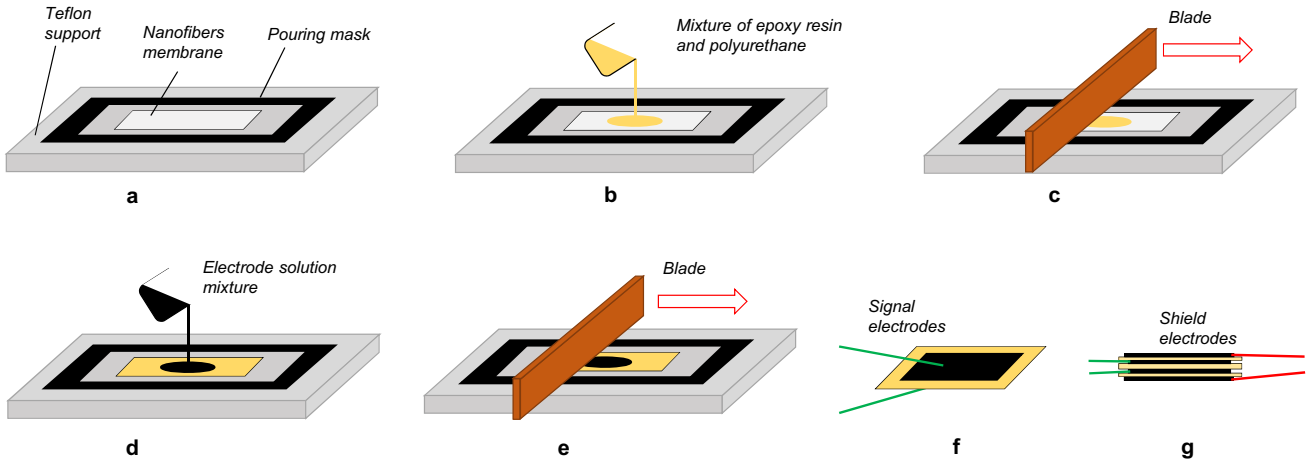

Fig. 4. Schematic representation of the piezoelectric sensor manufacturing process; (a) the nanofiber layer on a Teflon support; (b) pouring of epoxy resin and polyurethane mixture; (c) removal of the excess material and curing; (d) electrode solution mixture pouring; (e) removal of excess material; (f) piezoelectric sensor electrodes with signal cables; (g) addition of shield electrodes.

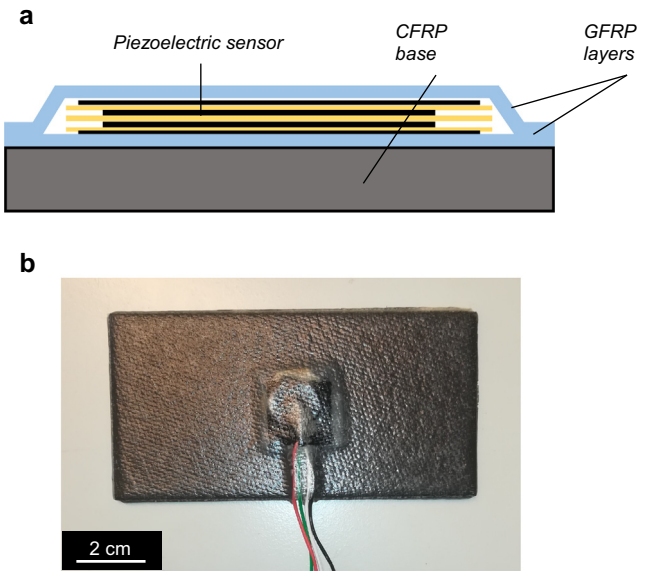

Fig. 5. (a) The stacking sequence of the self-sensing material; (b) the self-sensing laminate after the curing process.

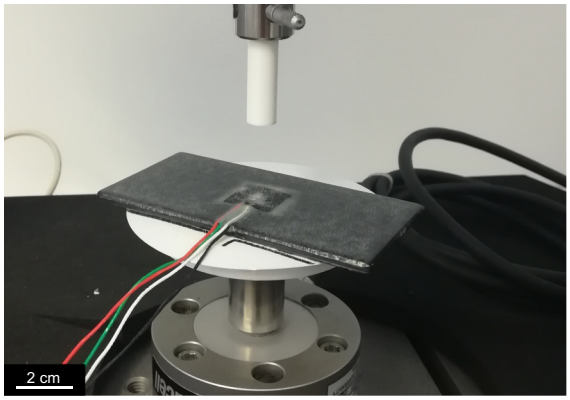

Fig. 6. Cyclic force indentation setup.

diameter of 1 cm, as shown in Fig. 6. The piezoelectric signal was conditioned by an AD795JRZ amplifier mounted on a single S08 precision amplifier evaluation board with a high-impedance input, and the shield electrodes were connected to the ground. The amplifier was set to the buffer mode, so no signal amplification was performed. Piezoelectric and load cell signals were synchronously acquired using a tensile machine. The piezoelectric response of the laminate was evaluated for different shunt resistances and capacitances connected in parallel to the amplifier input.

3. Results and discussion

The piezoelectric behavior of the self-sensing composite laminate is as follows: the micrograph analyses in Section 3.1 illustrate the adhesion between the piezoelectric sensor and GFRP layers. Furthermore, the piezoelectric model in Appendix B was experimentally validated using the electromechanical results described in Section 3.2. Finally, accelerated fatigue tests are performed (Section 3.3), and the results of the tests on a prosthetic sole incorporating three piezoelectric sensors are reported in Section 3.4.

3.1. Micrograph analyses

The use of nanofibers in a composite material is an established technique to increase the mode-I fracture toughness of the laminate and to reduce the risk of delamination owing to the intimate contact between each nanofiber and the epoxy matrix [35,36]. The morphology of the composite material in a cross-section was studied by optical microscopy and scanning electron microscopy (SEM). In the micrograph analysis in Fig. 7a, the stacking sequence can be observed with the [$CFRP_1$/$GFRP_1$/sensor/$GFRP_1$] sequence. As previously mentioned, the adhesion between the piezoelectric layer and the signal electrodes results from the use of the same epoxy matrix as a host material for both the integration of the nanofibers and dispersion of the carbon black nanoparticles. After polishing, the surface was immersed in an acetone bath for 1 h to dissolve the PVDF-TrFE nanofibers [22]. In this way, the removed nanofibers can be seen as holes in the SEM cross-sectional magnification of Fig. 7b, demonstrating the optimal embedding of the nanofibers into the epoxy matrix.

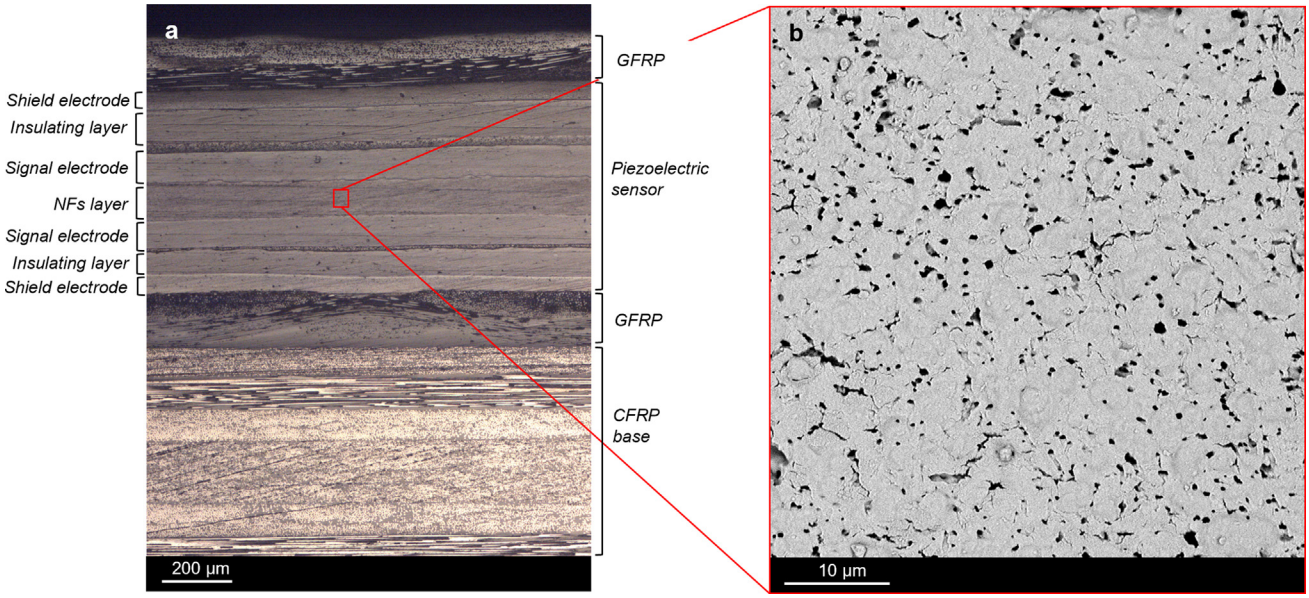

Fig. 7. (a) A micrograph image of a cross-section of the composite material; (b) An SEM image of the cross-section of the nanofibrous layer after etching in an acetone bath.

3.2. Electromechanical characterization

The variation in the RC constant of the equivalent electric circuit (Appendix B) results in different fittings of the piezoelectric curve to the applied force (F), along with different amplitudes of the output signal [22]. Fig. 8 shows the piezoelectric output signal of the sensor generated in response to a 200–500 N peak-to-peak compressive sinusoidal load at a frequency of 2 Hz, according to the setup described in Section 2.6. The *RC* constant of the circuit was varied by changing R_{load} and C_{load}, as described in Appendix B.

At low *RC* values (i.e., R_{load}=1 MΩ or R_{load} = 10 MΩ), derivative signal responses and improper matching of the piezoelectric output to the load-cell signal were observed. By increasing R_{load} to 1 GΩ and adding a capacitor (C_{load}) of 100 pF or 470 pF, the signal output of the sensor closely followed the load cell signal.

Moreover, changing the *RC* constant leads to a variation in the cutoff frequency f_c of the circuit. The sensitivity (mV/N) of the self-sensing laminate was studied as the ratio of the peak-to-peak value of the piezoelectric output voltage to the applied compressive force (F). A sinusoidal load oscillating between 200 and 500 N was applied to the sample for different frequencies and R_{load} values, as shown in Fig. 9a. The solid lines in the graph represent the theoretical values of the sensitivity, whereas the dots represent the experimental results.

The procedure for estimating the model predictions of the output voltage of the laminate involved calculation of the piezoelectric strain coefficient d_{33} of the self-sensing laminate, as reported in Appendix B. It is worth noting that the piezoelectric strain coefficient d_{33} of the laminate was equal to -36×10^{-3} pC/N. Compared to the coefficient of the original nanofiber membrane (−13 pC/N), the value of d_{33} being three orders of magnitude lower was due to the integration of the nanofibers with the hosting matrix (Fig. 4b) and the integration of the sensor into the composite laminate (Fig. 5), whose stiffness reduced the load transferred to the nanofibers and thus the generated charges.

The general trend of the graph in Fig. 9a shows a decrease in the f_c value with an increase in the *RC* constant, which is consistent with the model predictions (solid lines, Appendix B). In the cases where R_{load} is equal to 1 MΩ and 10 MΩ, the plateau region at 20 Hz was not reached (the frequency limit of the compression stiffness was 20 Hz). For each curve, the cutoff frequency f_c could be located in correspondence to a signal attenuation of 3 dB in the

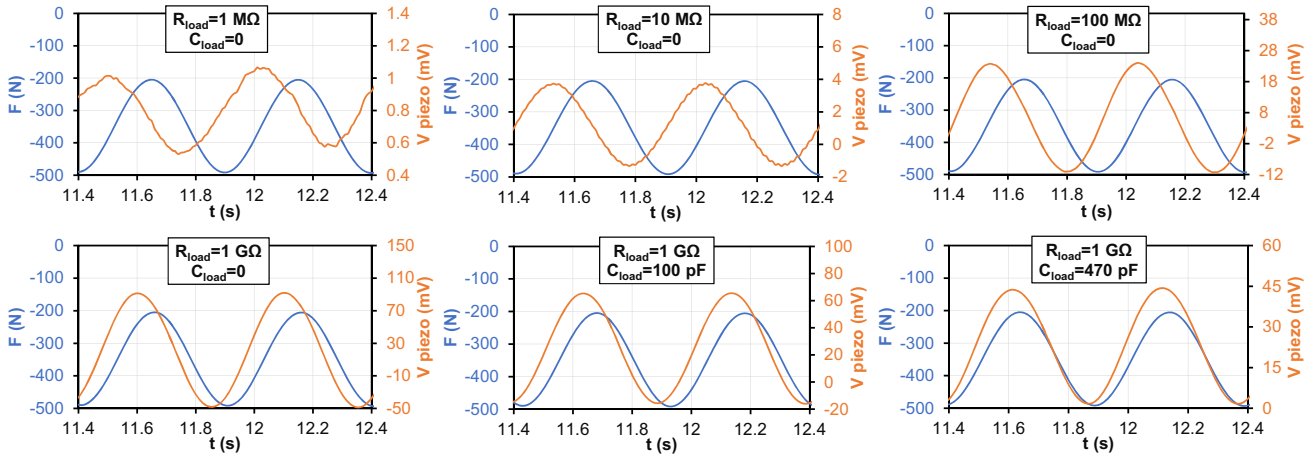

Fig. 8. The piezoelectric output signal (V) of the self-sensing laminate in response to a 2 Hz sinusoidal compression force (F) of 300 N for different values of R_{load} and C_{load}.

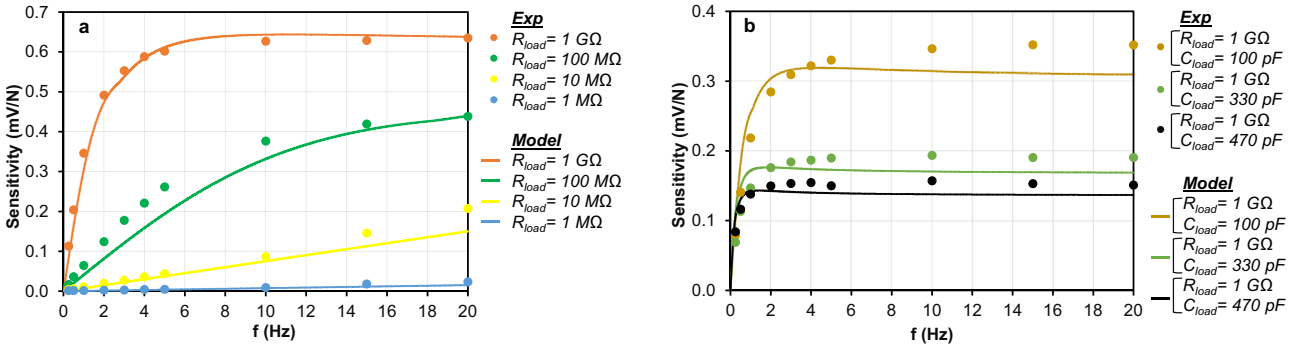

Fig. 9. (a) Sensitivity of the self-sensing laminate vs frequency for different R_{load} values; (b) sensitivity vs frequency for R_{load} = 1 GΩ and C_{load} varied (100 pF, 330 pF and 470 pF).

Bode diagram ($1/\sqrt{2}$ of the regime value). For R_{load} = 1 GΩ, the cut-off frequency was 1.67 Hz. Lower f_c values can be achieved only by connecting a capacitor (C_{load}) in parallel with R_{load} (set to 1 GΩ) to increase the RC constant of the circuit. In Fig. 9b, the sensitivity is reported at different frequencies for C_{load} set of 100, 330, and 470 pF. Generally, by adding capacitor C_{load} in parallel with R_{load}, the sensitivity can be attenuated. In the case of a 470 pF capacitor connected in parallel with a 1 GΩ resistor, the sensitivity was reduced by 76% and the cutoff frequency f_c dropped from 1.67 Hz to 0.52 Hz. This configuration makes the sensor suitable for low-frequency applications, such as ground reaction force detection in prosthetic systems, where the gait cycle period is approximately 1 s. For a suitable detection mechanism, the output voltage of the sensor must be proportional to the entire excitation frequency range.

For this configuration, a linearity analysis was performed by recording the piezoelectric peak-to-peak output voltage for different excitation force amplitudes. The frequency and lower peak force were set as 2 Hz and 200 N, respectively. Fig. 10 shows a sensitivity of 136.1 ± 3.3 mV/kN with a remarkably high coefficient of determination of 0.999 (R^2), which is typical for piezoelectric sensors.

3.3. Self-sensing laminate fatigue test

An accelerated cyclic fatigue test was performed on the self-sensing laminate by applying a sinusoidal load oscillating between 1000 and 400 N at a frequency of 10 Hz for 10^6 cycles, using the same setup as described in Section 2.6. The tests were performed at 20 °C. For accurate change detection, the R_{load} value was set to 1 GΩ and C_{load} = 0, the condition with the highest amplitude of

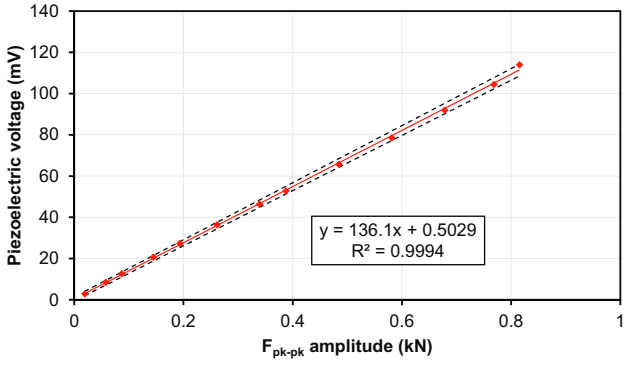

Fig. 10. Piezoelectric linearity test of the self-sensing laminate for R_{load} = 1 GΩ, and C_{load} = 470 pF.

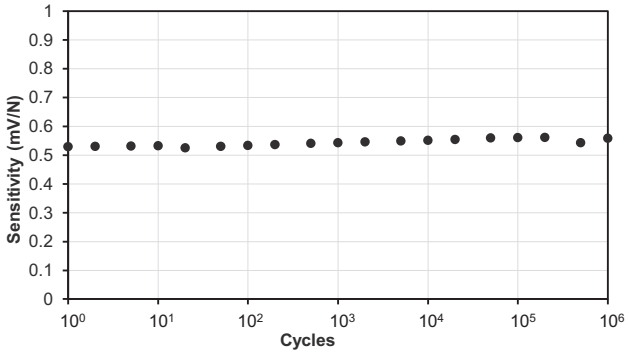

Fig. 11. A self-sensing laminate life cycle fatigue test, carried out at 10 Hz applying a sinusoidal load oscillating between 400 N and 1000 N.

the piezoelectric signal response. As shown in Fig. 11, the output voltage of the self-sensing laminate did not exhibit any significant fluctuations during the test and maintained its sensitivity over time.

3.4. Potential application fields

The flexible morphology of the manufactured piezoelectric sensor and the non-intrusiveness of the nanofibers on the host structure pave the way for a wide range of applications. In the field of robotics, piezoelectric nanofiber mats can be used as tactile sensors for prosthetic hands to create a network of pressure receptors in the fingers of the hand. The self-sensing capability of the laminate at low frequencies can be used to monitor quasi-static loads such as gripping-force control. In SHM systems, the piezoelectric self-sensing composite material combines the mechanical properties of the laminate with sensing capabilities that are not limited to damage detection but also enable in situ pressure monitoring. Owing to its flexibility, the sensor can be integrated into complex geometries and positioned remotely.

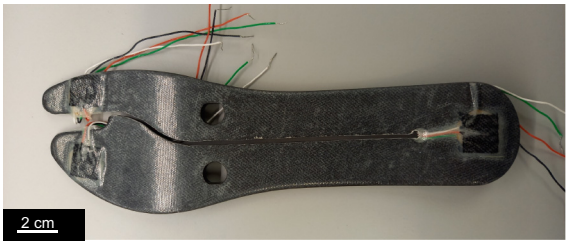

Fig. 12. Piezoelectric sensors integrated into a prosthetic sole.

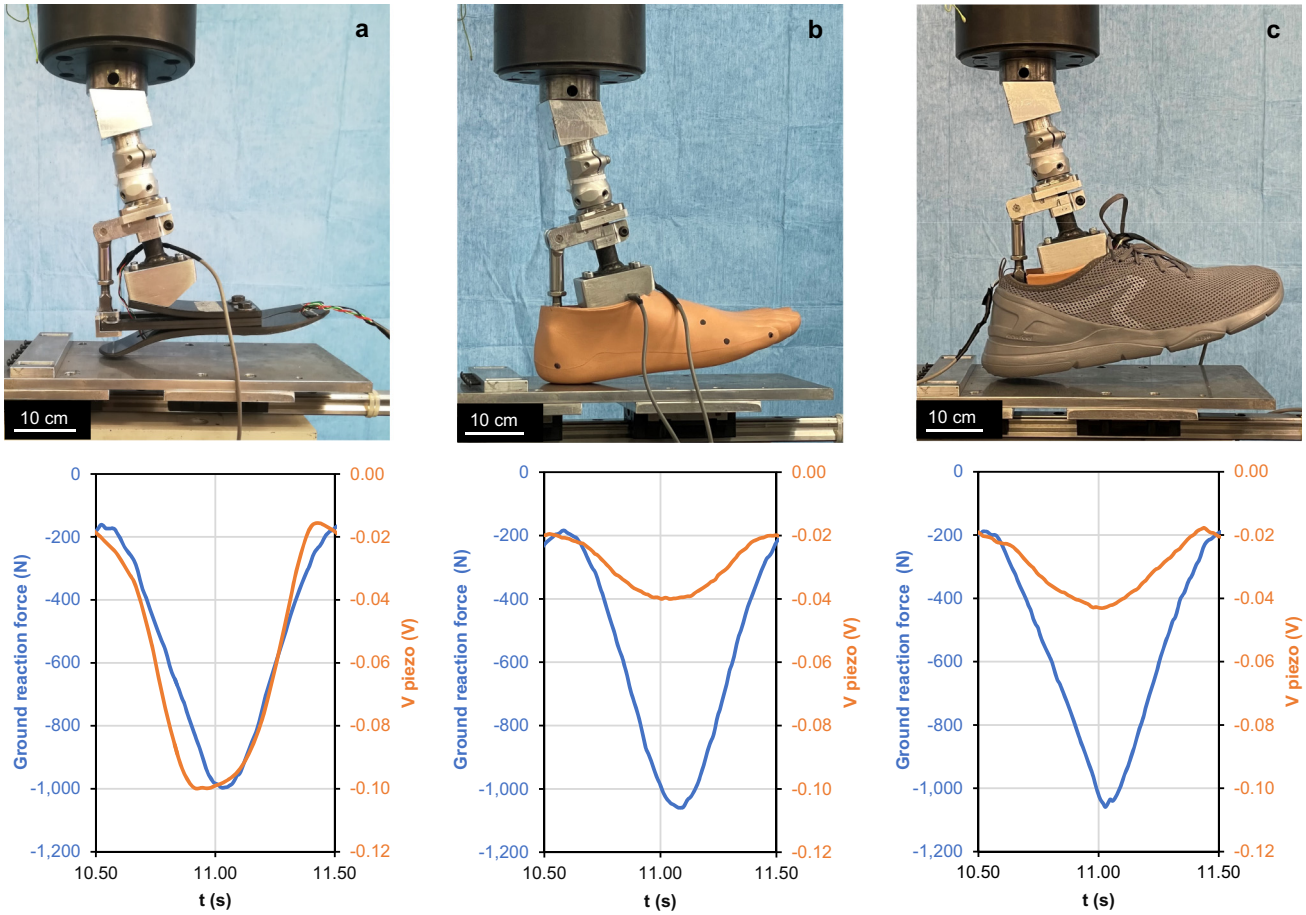

Fig. 13. Piezoelectric signal response of the sensor integrated into (a) the heel of the prosthetic sole; (b) with foot shell (c) and shoe mounted on it.

As a proof of concept, the fabricated sensors were embedded in the sole of a prosthetic foot. Two sensors were placed in the toe and one in the heel (Fig. 12), using the same stacking sequence described in Section 2.5. The piezoelectric signal response was acquired using the setup described in section 2.6. No amplification was performed during these tests; R_{load} was equal to 1 GΩ, and C_{load} was 470 pF.

The sole was then mounted on the ankle-foot prosthesis (Fig. 13), and compression tests were performed by applying a load to the heel oscillating between 200 and 800 N at a frequency of 1 Hz to mimic the period of the gait cycle. As can be observed in Fig. 13a, the piezoelectric signal closely followed the ground reaction force, with a sensitivity value of 0.11 mV/N, which is consistent with the behavior studied for the flat self-sensing specimen. Further analyses were performed using the same procedure by first placing the foot shell on the prosthetic foot and then the shoe, as shown in Fig. 13b and 13c. Indeed, prosthetic wearers usually wear a foot shell and often a shoe during their motor activities. It can be observed that the amplitude of the piezoelectric signal was reduced by 75% by the foot shell, and no further reductions were observed by adding the shoe.

4. Conclusions

The nanofiber flexible piezoelectric sensor was successfully integrated into a composite material. The nanofiber mat was embedded in a mixture of epoxy resin and polyurethane, compatible with the resin of the GFRP of the laminate, to avoid any risk of mechanical failure. In addition, the use of carbon black-based electrodes eliminated material discontinuities and increased the mechanical stability of the system. Although piezoelectric materials are traditionally used for dynamic loads, piezoelectric sensors can also accurately measure quasi-static loads by properly tuning the parameters of the electrical acquisition circuit. A sensitivity value of 0.14 ± 0.01 mV/N was found to be constant over a wide frequency range (from 0.5 Hz to 20 Hz), making the composite material suitable as a self-sensing device for a variety of applications. The measured linearity of the sensor had a coefficient of determination R^2 of 0.999. The sensitivity of the sensor was stable over 10^6 fatigue test cycles. Moreover, the flexible morphology of the piezoelectric sensor allowed suitable integration of the sensor into curvilinear geometries, such as a prosthetic foot sole. The piezoelectric signal response of the sensor embedded in the prosthesis was consistent with that of the sensor embedded in a flat composite laminate, demonstrating its feasibility for biomedical applications.

CRediT authorship contribution statement

Giacomo Selleri: Conceptualization, Methodology, Investigation, Formal analysis, Writing – original draft. **Maria Elena Gino:** Conceptualization, Methodology, Investigation, Formal analysis, Writing – original draft. **Tommaso Maria Brugo:** Conceptualization, Methodology, Investigation, Formal analysis, Writing – original draft. **Riccardo D'anniballe:** Conceptualization, Investigation. **Johnnidel Tabucol:** Conceptualization, Investigation. **Maria Letizia Focarete:** Conceptualization, Supervision. **Raffaella Carloni:** Conceptualization, Supervision. **Davide Fabiani:** Conceptualiza-

tion, Methodology, Investigation, Formal analysis, Writing – original draft. **Andrea Zucchelli:** Conceptualization, Supervision.

Data availability

The processed data required to reproduce these findings can be downloaded from [https://data.mendeley.com/datasets/y5k-st7j3t6/1].

Declaration of Competing Interest

The authors declare that they have no known competing financial interests or personal relationships that could have appeared to influence the work reported in this paper.

Acknowledgments

This research was funded by the European Union's Horizon 2020 Research and Innovation Programme – "MyLeg" (No. 780871, 2018) and was supported by the NATO Science for Peace and Security Programme (grant G5772). The authors thank Solvay and Ddchem S.l.r. for providing the polymers.

Appendix A

PVDF-TrFE is a semicrystalline copolymer that has been extensively studied for its piezoelectric and pyroelectric properties, which are inherently related to its structure. This copolymer has a complex structure and is characterized by the presence of different crystalline phases related to the different chain conformations that allow different packing of the dipoles within the unit cell. PVDF-TrFE was synthesized to possess an intrinsic β-phase that shows an all-TTTT conformation, where the polar C-F and C-H bonds possess a dipole moment perpendicular to the carbon backbone, making it the most electrically active phase [37]. In recent years, various techniques, including electrospinning, have been used to control and enhance the formation of the β-phase in PVDF-based polymers. During this process, both electrical and mechanical effects allowed the collection of β-phase rich fibers. Indeed, strong electrostatic uniaxial stretching introduced elongational forces in the direction of the jet, creating a molecular orientation which led to the transition from the α-phase to the β-phase [38]. The electrospun PVDF-TrFE nanofiber mat showed randomly oriented bead-free fibers with an average diameter of 420 ± 120 nm (Fig. 14a). The measured thickness of the mat was 100 ± 10 μm, and its areal weight was 20 g/m^2. To investigate the influence of the electrospinning process on the crystalline phase, the nanofibrous mat and PVDF-TrFE powder were analyzed using XRD, and the diffractograms of the two samples are shown in Fig. 14b. A prominent peak at 2θ = 19.8° was observed, representing the (200) Bragg reflections, which are typically assigned to the β-crystal phase of PVDF-TrFE, indicating that the ferroelectric phase was the dominant phase in the copolymer [39]. A shoulder centered around 18° was evident for the powder sample, attributed to a higher amount of amorphous material in the powder compared to the nanofibrous mat, as confirmed by the degree of crystallinity (48% for the powder and 58% for the electrospun fibers). This result indicates that the paraelectric phase of the copolymer decreased during the transition from powder to electrospun fibers, as indicated by the arrow in Fig. 14b.

Appendix B

The voltage output of the piezoelectric element was modeled by considering the piezoelectric transducer as a charge generator q_p. The equivalent electrical circuit of the self-sensing laminate connected to a voltage amplifier is represented in Fig. 15, where C_p is the capacitance of the piezoelectric element, R_p is its resistance, and C_c is the capacitance associated with the cables of the circuit. The two resistors R_{el} represent the semiconductive carbon black electrodes of the sensor, and the shunt resistor R_{load} provides a DC bias path for the amplifier input stage [26]. Capacitor C_{load} is added in parallel with resistor R_{load} before the amplifier input is used to tune RC constant of the circuit.

When an ideal capacitor is charged, voltage is stored owing to its infinite leakage resistance, which guarantees perfect insulation. However, because the internal resistance of the piezoelectric element is not infinite (R_p), the stored charges leak away, and the voltage drops exponentially at a rate determined by the time constant τ of the RC circuit, where $R = 2 * R_{el} + (R_{load} // R_p)$ and $C = C_p + C_c + C_{load}$. The capacitance of the piezoelectric layer was measured to be 55 pF, the capacitance of the cables was 5 pF, and the resistance of each semiconductive carbon-based electrode R_{el} was 4 kΩ.

By applying Kirchhoff's laws, the output voltage measured across R_{load} can be written as

$$V(t) = \frac{R}{j\omega RC + 1} d_{33} \frac{dF}{dt} \tag{3}$$

where, F is the applied force [22]. It can be noted that the output voltage is zero for static loads.

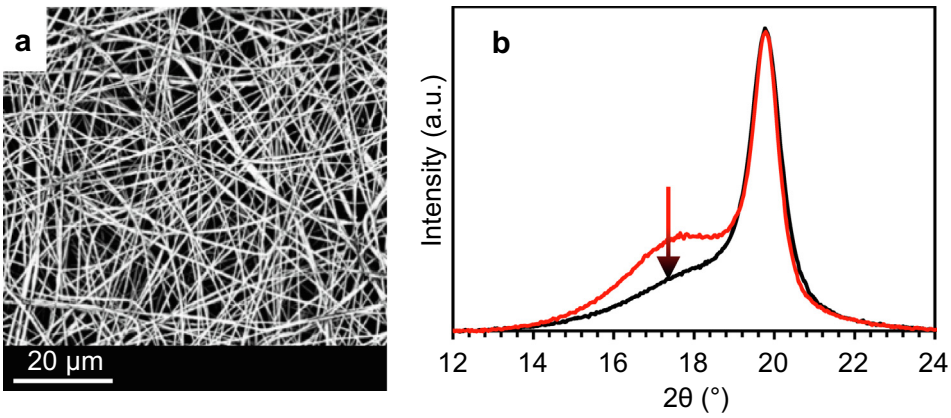

Fig. 14. Characterization of the nanofibrous piezoelectric mat of PVDF-TrFE; (a) SEM image; (b) XRD diffractograms of the electrospun membrane (black line) and powder before electrospinning (red line). (For interpretation of the references to colour in this figure legend, the reader is referred to the web version of this article.)

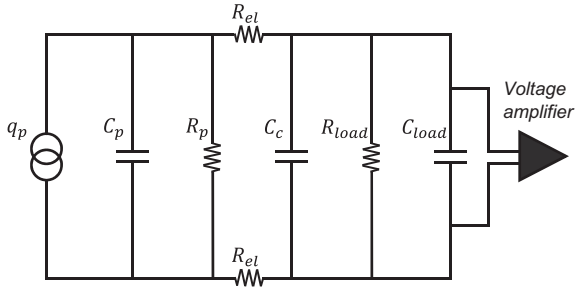

Fig. 15. The equivalent circuit of the piezoelectric sensor connected to a voltage amplifier.

In the case of a sinusoidal load $F(t) = F * \sin(\omega t)$, where $\omega = 2\pi/T$ and T is the period, Equation (3) can be solved in the Laplace domain and anti-transformed back in the time domain [22], as shown in Equation (4).

$$V(t) = \frac{F\omega R d_{33}}{\omega^2 R^2 C^2 + 1}\left(-e^{-t/RC} + \cos(\omega t) + \omega RC sin(\omega t)\right) \quad (4)$$

Moreover, by modeling the piezoelectric equivalent circuit as a series of voltage generators with equivalent capacitance C and resistance R, the resulting behavior of the circuit is equivalent to that of a high-pass filter, whose cutoff frequency depends on the RC time constant. To produce a self-sensing material that is capable of detecting quasi-static loads, the RC value must be appropriately tuned, for instance by increasing R_{load} or C_{load}. Indeed, a stable sensitivity value (ratio between the signal voltage and the applied force) over the entire frequency range guarantees linear behavior (signal voltage versus applied force) for an adequate detection mechanism even at low-frequency loads, such as the Gait cycle.

The d_{33} value of the piezoelectric element can be calculated using Equation (4). In the case of high RC values compared with the period of the applied force, which has an angular frequency ω - the exponential term and the first steady-state equation term can be neglected, and Equation (4) can be simplified as

$$V(t) = \frac{Fd_{33}}{C} sin(\omega t) \quad (5)$$

In the case of R_{load} equal to 1 GΩ, C_{load} equal to 100 pF, and the frequency of the compressive sinusoidal force equal to 20 Hz, the piezoelectric strain coefficient d_{33} of the self-sensing laminate was calculated by reversing Equation (5) and was equal to -36×10^{-3} pC/N.

References

[1] J. Leng, A. Asundi, Structural health monitoring of smart composite materials by using EFPI and FBG sensors, Sens. Actuators, A Phys. 103 (3) (2003) 330–340, https://doi.org/10.1016/S0924-4247(02)00429-6.

[2] P. Hofmann, A. Walch, A. Dinkelmann, S.K. Selvarayan, G.T. Gresser, Woven piezoelectric sensors as part of the textile reinforcement of fiber reinforced plastics, Compos. Part A Appl. Sci. Manuf. 116 (October 2018) (2019) 79–86, https://doi.org/10.1016/j.compositesa.2018.10.019.

[3] S. Rana, P. Subramani, R. Fangueiro, A.G. Correia, A review on smart self-sensing composite materials for civil engineering applications, AIMS Mater. Sci. 3 (2) (2016) 357–379, https://doi.org/10.3934/matersci.2016.2.357.

[4] L. D. Marchi, A. Perelli, N. Testoni, A. Marzani, D. Brunelli and L. Benini, "A small, light, and low-power passive node sensor for SHM of composite panels," in Proc. 9th International Workshop on Structural Health Monitoring, 2013, pp. 2325–2332

[5] U. Pierre Claver, G. Zhao, Recent Progress in Flexible Pressure Sensors Based Electronic Skin, Adv. Eng. Mater. 23 (5) (2021) 1–17, https://doi.org/10.1002/adem.202001187.

[6] Y. Wan, Y. Wang, C.F. Guo, Recent progresses on flexible tactile sensors, Mater. Today Phys. 1 (2017) 61–73, https://doi.org/10.1016/j.mtphys.2017.06.002.

[7] J. Hu, J. Yu, Y. Li, X. Liao, X. Yan, L. Li, Nano carbon black-based high performance wearable pressure sensors, Nanomaterials 10 (4) (2020), https://doi.org/10.3390/nano10040664.

[8] G. Schwartz, B.-K. Tee, J. Mei, A.L. Appleton, D.H. Kim, H. Wang, Z. Bao, Flexible polymer transistors with high pressure sensitivity for application in electronic skin and health monitoring, Nat. Commun. 4 (1) (2013), https://doi.org/10.1038/ncomms2832.

[9] Z. He, W. Chen, B. Liang, C. Liu, L. Yang, D. Lu, Z. Mo, H. Zhu, Z. Tang, X. Gui, Capacitive Pressure Sensor with High Sensitivity and Fast Response to Dynamic Interaction Based on Graphene and Porous Nylon Networks, ACS Appl. Mater. Interfaces 10 (15) (2018) 12816–12823.

[10] M.-S. Suen, R. Chen, Capacitive Tactile Sensor with Concentric-Shape Electrodes for Three-Axial Force Measurement, Proceedings 2(13) (2018) 708, doi: 10.3390/proceedings2130708.

[11] J. Shintake, E. Piskarev, S.H. Jeong, D. Floreano, Ultrastretchable Strain Sensors Using Carbon Black-Filled Elastomer Composites and Comparison of Capacitive Versus Resistive Sensors, Adv. Mater. Technol. 3 (3) (2018) 1–8, https://doi.org/10.1002/admt.201700284.

[12] A. Ahmed et al., Triboelectric Nanogenerator versus Piezoelectric Generator at Low Frequency (<4 Hz): A Quantitative Comparison, *iScience* 23(7) (2020), doi: 10.1016/j.isci.2020.101286.

[13] F.R. Fan, Z.Q. Tian, Z. Lin Wang, Flexible triboelectric generator, Nano Energy 1 (2) (2012) 328–334, https://doi.org/10.1016/j.nanoen.2012.01.004.

[14] K.-I. Park, J.H. Son, G.-T. Hwang, C.K. Jeong, J. Ryu, M. Koo, I. Choi S.H. Lee, M. Byun, Z.L. Wang, K.J. Lee, Highly-efficient, flexible piezoelectric PZT thin film nanogenerator on plastic substrates, Adv. Mater. 26 (16) (2014) 2514–2520.

[15] A. Al-Saygh, D. Ponnamma, M.A.A. AlMaadeed, P. Poornima Vijayan, A. Karim, M.K. Hassan, Flexible pressure sensor based on PVDF nanocomposites containing reduced graphene oxide-titania hybrid nanolayers, Polymers (Basel) 9 (2) (2017) 33, https://doi.org/10.3390/polym9020033.

[16] H. Yuan, T. Lei, Y. Qin, R. Yang, Flexible electronic skins based on piezoelectric nanogenerators and piezotronics, Nano Energy 59 (October 2018) (2019) 84–90, https://doi.org/10.1016/j.nanoen.2019.01.072.

[17] J. Chang, Y. Shen, X. Chu, X. Zhang, Y.u. Song, Y. Lin, C.-W. Nan, L. Li, Large d33 and enhanced ferroelectric/dielectric properties of poly(vinylidene fluoride)-based composites filled with Pb(Zr0.52Ti0.48)O3 nanofibers, RSC Adv. 5 (63) (2015) 51302–51307.

[18] J. Liu et al., Flexible and lead-free piezoelectric nanogenerator as self-powered sensor based on electrospinning BZT-BCT/P(VDF-TrFE) nanofibers, Sens. Actuators, A Phys. 303 (2020) 111796, https://doi.org/10.1016/j.sna.2019.111796.

[19] J. Cheng, C. Qian, M. Zhao, S.W.R. Lee, P. Tong, T.Y. Zhang, Effects of electric fields on the bending behavior of PZT-5H piezoelectric laminates, Smart Mater. Struct. 9 (6) (2000) 824–831, https://doi.org/10.1088/0964-1726/9/6/312.

[20] B. Yang, F.-Z. Xuan, P. Jin, C. Hu, B. Xiao, D. Li, Y. Xiang, H. Lei, Damage Localization in Composite Laminates by Building in PZT Wafer Transducers: A Comparative Study with Surface-Bonded PZT Strategy, Adv. Eng. Mater. 21 (3) (2019) 1801040.

[21] T. Brugo, R. Palazzetti, The effect of thickness of Nylon 6,6 nanofibrous mat on Modes I-II fracture mechanics of UD and woven composite laminates, Compos. Struct. 154 (2016) 172–178, https://doi.org/10.1016/j.compstruct.2016.07.034.

[22] T.M. Brugo, E. Maccaferri, D. Cocchi, L. Mazzocchetti, L. Giorgini, D. Fabiani, A. Zucchelli, Self-sensing hybrid composite laminate by piezoelectric nanofibers interleaving, Compos. Part B Eng. 212 (2021) 108673.

[23] G. Moretti, M. Righi, R. Vertechy, M. Fontana, Fabrication and test of an inflated circular diaphragm dielectric elastomer generator based on PDMS rubber composite, Polymers (Basel) 9 (7) (2017) 283, https://doi.org/10.3390/polym9070283.

[24] G. Selleri, D. Fabiani, A. Zucchelli, T.M. Brugo, F. Grolli, L. Bordoni, Develompment of flexible sensors based on piezoelectric nanofibers, Proc. IEEE Int. Conf. Prop. Appl. Dielectr. Mater. 20-July (Icpadm) (2021) 358–361, https://doi.org/10.1109/ICPADM49635.2021.9493957.

[25] M. Tavakoli, R. Rocha, L. Osorio, M. Almeida, A. de Almeida, V. Ramachandran, A. Tabatabai, T. Lu, C. Majidi, Carbon doped PDMS: conductance stability over time and implications for additive manufacturing of stretchable electronics, J. Micromech. Microeng. 27 (3) (2017) 035010.

[26] M. Serridge, T.R. Licht, Piezoelectric Accelerometers and Vibration Preamplifiers: Theory and Application Handbook, Bruel & Kjaer, 1987.

[27] F. Calavalle, M. Zaccaria, G. Selleri, T. Cramer, D. Fabiani, B. Fraboni, Piezoelectric and Electrostatic Properties of Electrospun PVDF-TrFE Nanofibers and their Role in Electromechanical Transduction in Nanogenerators and Strain Sensors, Macromol. Mater. Eng. 305 (7) (2020) 1–8, https://doi.org/10.1002/mame.202000162.

[28] H.L.W. Chan, Z. Zhao, K.W. Kwok, C.L. Choy, C. Alquié, C. Boué, J. Lewiner, Polarization of thick polyvinylidene fluoride/trifluoroethylene copolymer films, J. Appl. Phys. 80 (7) (1996) 3982–3991.

[29] G. Eberle, E. Bihler, W. Eisenmenger, Polarization Dynamics of VDF-TrFE Copolymers, IEEE Trans. Electr. Insul. 26 (1) (1991) 69–77, https://doi.org/10.1109/14.68230.

[30] H. Naderiallaf, P. Seri, G.C. Montanari, Designing a HVDC Insulation System to Endure Electrical and Thermal Stresses under Operation. Part I: Partial Discharge Magnitude and Repetition Rate during Transients and in DC Steady State, IEEE Access 9 (2021) 35730–35739, https://doi.org/10.1109/ACCESS.2021.3062440.

[31] G. Selleri et al., Study on the polarization process for piezoelectric nanofibrous layers, IEEE Conf. Electr. Insul. Dielectr. Phenom. (2021) 31–34.
[32] H. Naderiallaf, P. Seri, G. Montanari, On the calculation of the dielectric time constant of DC insulators containing cavities, IEEE Conf. Electr. Insul. Dielectr. Phenom. (2021) 668–671.
[33] H.J. Choi, M.S. Kim, D. Ahn, S.Y. Yeo, S. Lee, Electrical percolation threshold of carbon black in a polymer matrix and its application to antistatic fibre, Sci. Rep. 9 (1) (2019) 1–12, https://doi.org/10.1038/s41598-019-42495-1.
[34] L. Lu, D.i. Xing, Y. Xie, K.S. Teh, B. Zhang, S. Chen, Y. Tang, Electrical conductivity investigation of a nonwoven fabric composed of carbon fibers and polypropylene/polyethylene core/sheath bicomponent fibers, Mater. Des. 112 (2016) 383–391.
[35] H. Zarei, T. Brugo, J. Belcari, H. Bisadi, G. Minak, A. Zucchelli, Low velocity impact damage assessment of GLARE fiber-metal laminates interleaved by Nylon 6,6 nanofiber mats, Compos. Struct. 167 (2017) 123–131, https://doi.org/10.1016/j.compstruct.2017.01.079.
[36] H. Saghafi, T. Brugo, G. Minak, A. Zucchelli, The effect of PVDF nanofibers on mode-I fracture toughness of composite materials, Compos. Part B Eng. 72 (2015) 213–216, https://doi.org/10.1016/j.compositesb.2014.12.015.
[37] P. Martins, A.C. Lopes, S. Lanceros-Mendez, Electroactive phases of poly (vinylidene fluoride): Determination, processing and applications, Prog. Polym. Sci. 39 (4) (2014) 683–706, https://doi.org/10.1016/j.progpolymsci.2013.07.006.
[38] J. Zheng, A. He, J. Li, C.C. Han, Polymorphism control of poly(vinylidene fluoride) through electrospinning, Macromol. Rapid Commun. 28 (22) (2007) 2159–2162, https://doi.org/10.1002/marc.200700544.
[39] S. Park, Y. Kwon, M. Sung, B.S. Lee, J. Bae, W.R. Yu, Poling-free spinning process of manufacturing piezoelectric yarns for textile applications, Mater. Des. 179 (2019), https://doi.org/10.1016/j.matdes.2019.107889 107889.